Elucidation of Pathophysiological Factors of Cardiovascular Diseases

Naoki Kobayashi*, Kento Morita*,†, Nice Ren†, Shogo Watanabe†,
Syoji Kobashi†,‡, Kinta Hatakeyama†, Koji Iihara†, Tetsushi Wakabayashi*

*Graduate School of Engineering, Mie University, Mie, Japan
†National Cerebral and Cardiovascular Center, Osaka, Japan
‡Graduate School of Engineering, University of Hyogo, Hyogo, Japan

E-MAIL: 424M510@m.mie-u.ac.jp

Abstract:

Cardiovascular diseases are the second leading cause of death in Japan, underscoring the need for improved prevention and treatment. Carotid endarterectomy (CEA) is a surgical procedure to remove plaque that has accumulated in the intima of the carotid artery, and is expected to reduce the risk of stroke. However, the long-term prognosis and complications after CEA surgery are not fully understood. In this study, we investigate pathological factors associated with the modified Rankin Scale (mRS) score, based on features extracted from pathological images of plaques removed by CEA and clinical data.

We extract features from pathological images using an autoencoder (AE) and analyze them with Lasso regression to investigate their association with the mRS score. The obtained R^2 score was 0.8427, suggesting that the features obtained by AE retained sufficient information related to the mRS score. It should be noted that this analysis was conducted on the training set; therefore, its generalization performance needs to be evaluated in the future. We also visualized the regions associated with the mRS score in pathological images using the trained regression model.

Keywords:

Carotid Endarterectomy (CEA), modified Rankin Scale (mRS), Outcome Prediction

1. Introduction

In Japan, cardiovascular disease is the second leading cause of mortality, following cancer. Although many studies have investigated the disease's pathogenesis and aimed to develop preventive and therapeutic approaches [1], no effective treatment has been established yet [2]. CEA is a surgical procedure that removes plaque from the intima of the carotid artery. It is performed to reduce the risk of stroke caused by atherosclerosis-induced narrowing and reduced blood flow to the brain. The carotid artery serves as a major conduit for blood flow to both the heart and brain. When plaque accumulates within the artery, it can lead to a deterioration in cerebral blood flow. In some cases, the plaque may rupture, resulting in a stroke. CEA is a surgical procedure performed to remove such plaque and has been shown to reduce the incidence of stroke [3]. However, the long-term outcomes of this procedure remain uncertain. According to Ref. [4], between 6% and 36% of patients who undergo CEA may experience restenosis, which limits the procedure's long term efficacy. Although there are existing studies that have used ultrasound echocardiographic images of patients [5] and clinical data from patients [6]~[8] to predict prognosis after CEA surgery, there are no studies that have examined the relationship between carotid plaque pathology and postoperative outcomes. In this paper, we perform data mining to predict outcomes after CEA using features extracted from pathological images of plaques removed by CEA. We also estimate the regions in the pathological images that contributed to the prediction by visualization with heat maps.

2. Preliminaries

2.1 Dataset

The study uses pathological images and clinical data from 141 cases collected at the National Cerebral and Cardiovascular Center. The cases include patients with

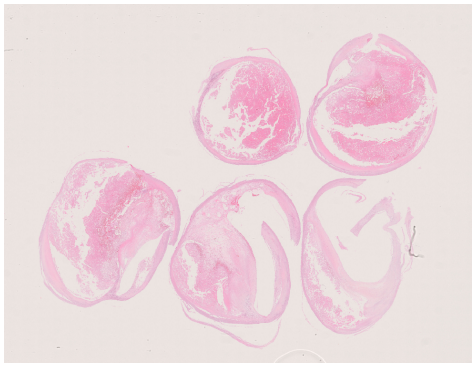

FIGURE 1. An example of a pathological image

TABLE 1. Patient Distribution by mRS Score. The mRS categorizes functional outcomes as follows: 0 = No symptoms, 1 = No significant disability, able to carry out all usual activities, 2 = Slight disability, unable to carry out all previous activities but able to look after own affairs without assistance, 3 = Moderate disability, requiring some help but able to walk unassisted, 4 = Moderately severe disability, unable to walk and attend to bodily needs without assistance, 5 = Severe disability, bedridden, requiring constant nursing care [9]

mRS	0	1	2	3	4	5
Patients	72	36	13	11	3	3

carotid artery stenosis, and pathological evaluation was performed by a certified pathologist. Pathological images are Whole Slide Imaging (WSI) of hematoxylin and eosin (H&E) stained specimens taken with a 40× magnification (Fig. 1).

mRS is used as an index to evaluate the clinical outcome of patients. It is defined on a 6-point scale ranging from 0 to 5, and is commonly used to assess a patient's functional prognosis. Table 1 shows the number of patients for each mRS grade.

The study was approved by the Ethics Committee of the National Cerebral and Cardiovascular Center, and informed consent was obtained from the patients.

2.2 Autoencoder [10]

Autoencoder (AE) is a type of neural network for data compression and feature extraction. The structure consists of two parts, an encoder and a decoder. The encoder compresses the input data into a low-dimensional latent space, while the decoder reconstructs the original data from this representation. The network learns by minimizing the difference between the input and the reconstructed data, thereby updating the weights of both the encoder and decoder. This yields a low-dimensional latent representation of the data. Since the architecture of the encoder, decoder, and loss function can be freely designed, the model can be tailored to fit the specific characteristics of the data. In this study, only the encoder is utilized as a feature extraction model after training the AE to accurately reconstruct the input data.

2.3 Lasso regression

Lasso regression (Least Absolute Shrinkage and Selection Operator) is a linear regression technique that incorporates an L^1 regularization term, promoting sparsity in the regression coefficients. The L^1 regularization enhances model interpretability by performing feature selection and retaining only the most relevant variables. During the learning process, a linear combination of the input data is computed. The regression coefficients are then iteratively updated to minimize the difference between the predicted results and the target variable. The regression coefficients are updated by minimizing an objective function that includes an L^1 regularization term. L^1 regularization penalizes the sum of the absolute values of the coefficients, effectively shrinking those with small contributions to zero. This allows Lasso regression to reduce unnecessary features and sparsify the model.

3. Proposed Method

In this study, we focus on carotid plaques extracted via CEA and aim to evaluate the association between image-derived features and clinical outcomes (mRS). The proposed method follows the process shown in Fig. 2. First, the pathological image is segmented. Next, patches of 256×256 pixels are extracted from the segmented image. These patches are processed with a pre-trained AE to extract feature vectors. The feature vectors for each patient are then averaged to form a representative vector. The representative vector is input into a Lasso regression model to predict the mRS score. Finally, post-processing such as rounding and clipping is performed to obtain the mRS score.

3.1 WSI processing

Due to the large size of pathological images, direct analysis using CNN models is computationally expensive and

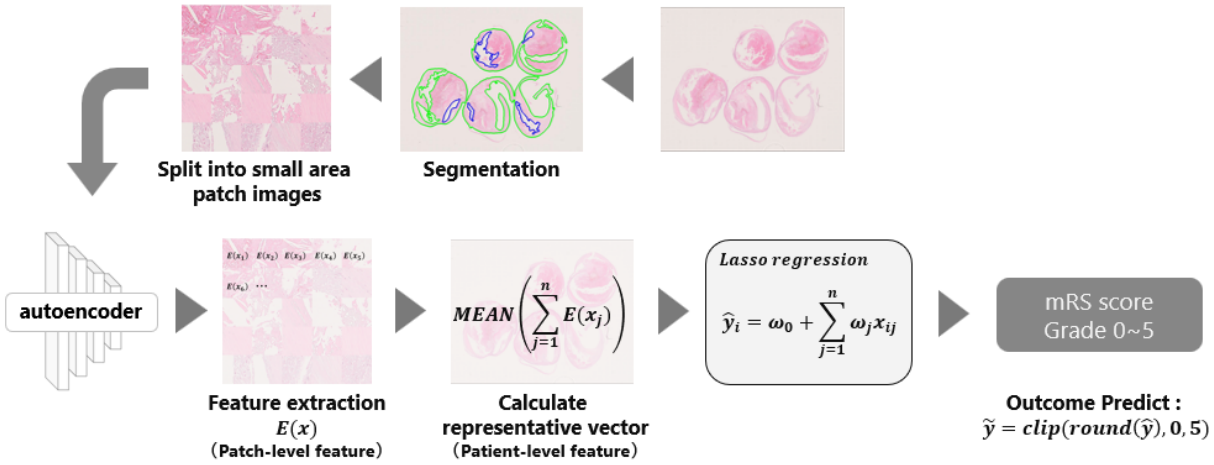

FIGURE 2. Proposed method overview

memory-intensive. Therefore, in this study, we preprocess WSIs using CLAM (Clustering-constrained Attention Multiple Instance Learning) [11] to segment plaques in WSIs and extract 256 × 256 pixels patches by the sliding window. In addition, patches containing more than 30% of pixels with RGB values in the range from [220, 220, 220] to [255, 255, 255] are removed to eliminate those with excessive background.

3.2 Prior training of autoencoder

The encoder part of the AE is used to obtain a feature representing the pathological feature representation of the patch image with pathological features of the pathological image. Patch images from patients randomly sampled from the entire dataset are used to train the AE. The encoder architecture takes a 256 × 256 × 3 patch image as input and outputs a 16 × 16 × 256 latent representation. The encoder architecture consists of four convolutional and pooling layers, while the decoder comprises four transposed convolutional layers.

3.3 Feature extraction

By using the encoder part of the trained autoencoder, pathological image features are extracted from patch images. Since the extracted features are obtained on a per-patch basis, feature vectors are averaged to generate a representative vector for each patient. These representative vectors are then used for subsequent regression analysis.

3.4 Pathological feature analysis for the mRS prediction

In this study, we aim to investigate the relationship between pathological features extracted from WSI and the clinical outcome, measured as the mRS. Given the limited sample size, we prioritize uncovering potential trends rather than constructing a robust predictive model. To achieve this, we employ Lasso regression, which is well-suited for small datasets and feature selection due to its L^1 regularization property.

Lasso regression models the relationship between each patient's representative feature vector x_i and the corresponding mRS score y_i as a linear combination, as described in Eq.(1).

$$\hat{y}_i = w_0 + \sum_{j=1}^{n} w_j x_{ij} \tag{1}$$

The model is trained by minimizing the objective function in Eq.(2), which includes both the squared error and an L^1 regularization term to enforce sparsity.

$$L(w) = \frac{1}{2N} \sum_{i=1}^{N} (y_i - \hat{y}_i)^2 + \alpha \sum_{j=1}^{n} |w_j| \tag{2}$$

where N is the number of patients, n is the dimensionality of the representative vector, $\hat{y}_i$ is the predicted mRS score, y_i is the ground truth mRS score, and α is a hyperparameter that controls the strength of the regularization.

TABLE 2. Lasso regression training data distribution

mRS			0	1	2	3	4	5
Patients	AE	train	4	0	0	0	1	0
		valid	1	0	0	0	0	0
	Lasso	train	13	13	13	11	2	3

During training, regression coefficients w_j are adjusted to minimize the difference between $\hat{y}_i$ and y_i, with the L^1 penalty shrinking coefficients with low contributions toward zero. This results in a sparse model that highlights features contributing to predicting the mRS score. Since Lasso regression yields continuous values, the predicted mRS values are constrained by rounding and clipping to the range of 0 to 5.

4 Experiment

4.1 Experimental dataset

Due to the limited number of available samples, different data subsets were selected for training the AE and the Lasso regression model, each tailored to its specific analytical objective. For AE training, patch images were sampled from five randomly selected patients.

This approach aims to ensure sufficient generalization performance of the encoder using a minimal dataset. Patch images from one additional patient are used for validation. To prevent data leakage, patients used in AE training are excluded from the Lasso regression dataset.

For Lasso regression, stratified random sampling is applied to maintain class balance across mRS scores and to suppress the decline in learning accuracy caused by data imbalance. Up to 13 patients were selected per class, based on the number of patients in the third most frequent class (mRS = 2). Table 2 summarizes the number of patients used for AE training, AE validation, and Lasso regression.

4.2 Autoencoder training

The AE is trained with the following parameters: the batch size is set to 64, Adam [12] with a learning rate of 0.001 is used as the optimizer, the L^2 loss is utilized as the loss function, and the number of epochs is set to 50 to prevent overfitting.

Figure 3 shows an example of the reconstruction when the data for evaluation is input. After comparing before and after reconstruction, we determined that the generalization performance was satisfactory, so we will use the learned AE in subsequent experiments.

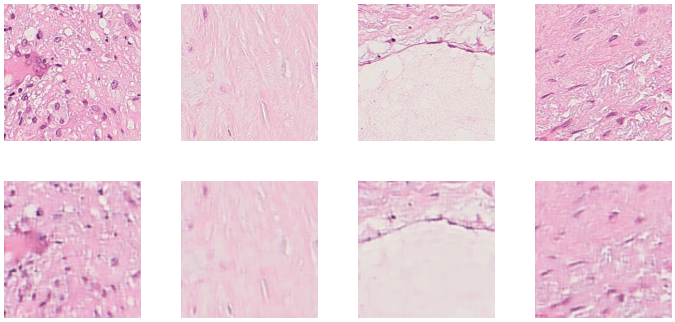

FIGURE 3. Comparison of original input patches (top row) and corresponding reconstructed patches (bottom row).

4.3 Lasso regression and heat-map analysis

The Lasso regression is trained using the following parameters: the regularization term weight is set to 0.1, and the maximum number of iterations is 10,000 to ensure convergence. The model's performance is evaluated using the coefficient of determination (R^2), which quantifies the agreement between the predicted values and the ground truth mRS scores. An R^2 value closer to 1 indicates better model explanatory power.

In this analysis, the Lasso regression achieved an R^2 score of 0.8427, suggesting that the trained model effectively captured pathological features related to mRS scores. It is considered that the features from pathological images adequately reflect the differences in mRS and that the regression analysis is able to extract their relevance. These results indicate that the image-derived features sufficiently reflect inter-patient differences in mRS, and that Lasso regression successfully modeled their relationship.

To further examine the model's predictive behavior, a confusion matrix is generated by discretizing the continuous prediction outputs. As shown in Fig. 4, the model achieved particularly high accuracy for mRS scores of 1 and 2, indicating strong predictive performance in these categories. Furthermore, most misclassifications occurred between adjacent mRS classes, reflecting the ordinal nature of the mRS scale. This pattern suggests that the model captures the gradation of functional severity and demonstrates its potential to make clinically meaningful estimations from pathology-derived features.

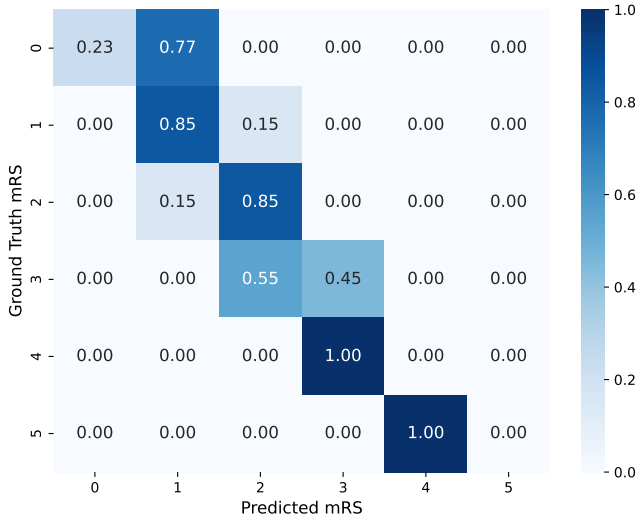

FIGURE 4. Confusion matrix of predicted vs. ground truth mRS scores.

Additionally, a heatmap is created to visualize the predictive score of the Lasso regression for pathological images using the learned regression model. An example is shown in Fig. 5, with brighter colors in the heat-map indicating higher scores. These visualizations revealed regions with concentrated high prediction values across multiple images. If such high-scoring regions correspond to known pathological abnormalities or specific tissue distributions, this method could provide insights into the associations between localized pathological features and clinical outcomes such as the mRS.

5. Conclusions

In this paper, data mining is performed to predict the mRS score, which represents patient outcomes, based on features extracted from pathological images. Features are extracted from pathological images using an AE and analyzed using Lasso regression to investigate the relationship between the images and mRS scores. The obtained R^2 score was as high as 0.8427, suggesting that the features extracted through AE retained relevant information related to the mRS. However, they may reflect local patterns that are overfit to the training data, and future studies should evaluate the generalization performance of models using different datasets. Additionally, heatmaps created using the learned regression model identify areas of concentration of high-scoring regions in pathological images. This demonstrates the potential for analyzing the association between pathological images and clinical indicators. We believe that the results of this paper provide a basis for predicting patient prognosis from pathological images and help to better understand the relationship between pathological features and clinical factors.

References

[1] C. Ruiz-Carmona, C. Diaz-Duran, N. Sevilla, E. Cuadrado, and A. Clara, "Long-term survival after carotid endarterectomy in a population with a low coronary heart disease fatality: Implications for decision making," Annals of Vascular Surgery, vol. 36, 2016.

[2] S. Shimoda, A. Kitamura, H. Imano, R. Cui, I. Muraki, K. Yamagishi, M. Umesawa, T. sankai, M. Hayama-Terada, Y. Kubota, Y. Shimizu, T. Okada, M. Kiyama, and H. Iso, "Associations of carotid intima-media thickness and plaque heterogeneity with the risks of stroke subtypes and coronary artery disease in the japanese general population: The circulatory risk in communities study," J Am Heart Assoc, vol. 9, no. 19, p. e17020, 2020.

[3] T. Konishi, N. Funayama, T. Yamamoto, T. Morita, D. Hotta, R. Nomura, Y. Nakagaki, T. Murahashi, K. Kamiyama, T. Yoshimoto, T. Aoki, H. Nishihara, and S. Tanaka, "Pathological quantification of carotid artery plaque instability in patients undergoing carotid endarterectomy," Circulation Journal, vol. 82, no. 1, pp. 258–266, 2018.

[4] L.H. Bonati, J. Gregson, J. Dobson, D.J.H. McCabe, P.J. Nederkoorn, H.B. van der Worp, et al., "Restenosis and risk of stroke after stenting or endarterectomy for symptomatic carotid stenosis in the International Carotid Stenting Study (ICSS): secondary analysis of a randomised trial," Lancet Neural, 17(2018), pp. 587-596

[5] Y. Kokubo, M. Wanatabe, A. Higashiyama, Y. Nakao, F. Nakamura, and Y. Miyamoto, "Impact of intima-media thickness progression in the common carotid arteries on the risk of incident cardiovascular disease in the suita study," J Am Heart Assoc, vol. 7, no. 11, p. e007720, 2018.

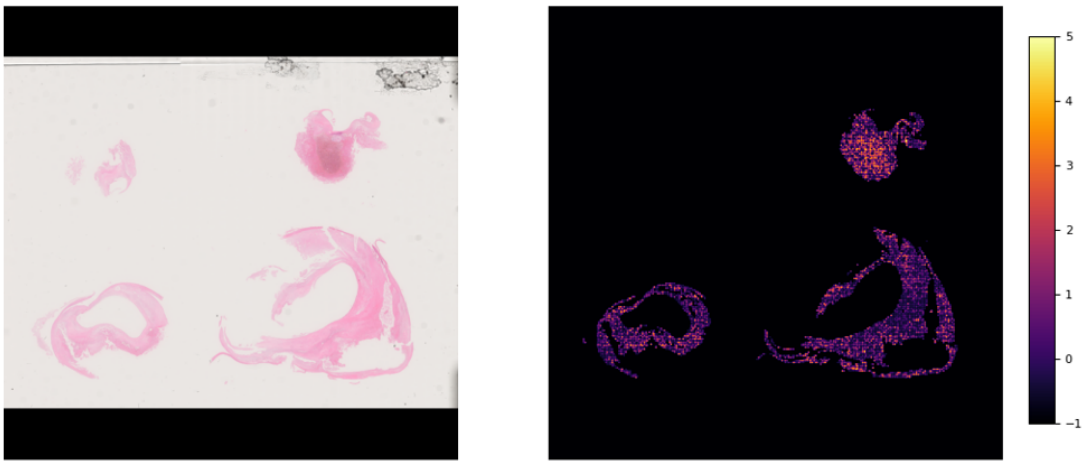

FIGURE 5. Heat-map (original image on the left, heat-map on the right) In the upper right pathological area, high scores are concentrated.

[6] A. Matsuo, A. Fujita, K. Hosoda, J. Tanaka, T. Imahori, M. Ishii, Tanmd Kohta, K. Tanaka, Y. Uozumi, H. Kimura, T. Sasayama, and E. Kohmura, "Potential of machine learning to predict early ischemic events after carotid endarterectomy or stenting: a comparison with surgeon predictions," Neurosurg Rev, vol. 45, no. 1, pp. 607–616, 2022.

[7] B. Li, D. Beaton, N. Eisenberg, D. Lee, D. Wijeysunder, T. Lindsaym, C. de Mastral, C. Roche-Nagle, and M. AI-Omran, "Using machine learning to predict outcomes following carotid endarterectomy," J Vasc Surg, vol. 78, no. 4, pp. 973–987.e6, 2023.

[8] B. Li, R. Verma, D. Beaton, H. Tamim, M. Hussain, J. Hoballah, D. Lee, D. Wijeysundera, C. de Mastral, M. Mamdani, and H. AI-Omran, "Predicting major adverse cardiovascular events following carotid endarterectomy using machine learning," J Am Heart Assoc, vol. 12,no. 20, p. e030508, 2023.

[9] Y. Shinohara, K. Minematsu, T. Amano, Y. Ohashi, "Reliability of modified Rankin Scale," Jpn J Storoke, 29:6-13,2007

[10] G. E. Hinton, and R. R. Salakhutdinov, "Reducing the dimensionality of data with neural networks. Science," Vol. 313, No. 5786, pp. 504–507, 2006.

[11] M. Lu, D. Williamson, T. Chen, R. Chen, M. Barbieri, F. Mahmood, "Data Efficient and Weakly Supervised Computational Pathology on Whole Slide Images," Nature biomedical engineering 5.6 (2021): 555-570

[12] Kingma, P. Diederik, and B. Jimmy, "Adam: A method for stochastic optimization," International Conference on Learning Representations, 2015.